The following publication K. Huang, H. K. Chu, B. Lu and L. Cheng, "Characterization of a Microchip Device for Cell Patterning via Negative Dielectrophoresis," 2018 IEEE International Conference on Robotics and Biomimetics (ROBIO), 2018, pp. 1521-1526 is available at https://doi.org/10.1109/ROBIO.2018.8665210.

Characterization of a Microchip Device for Cell Patterning via Negative Dielectrophoresis

Kaicheng Huang, Henry K. Chu*, *Member, IEEE*, Bo Lu and Li Cheng

***Abstract*— Patterning cells on a substrate is useful for cell assay and characterization. In this paper, a microchip employing negative dielectrophoresis was designed for efficient cell pattering. This chip consists of a 4-by-4 dot electrode array and the cell patterns are formed on a substrate lying on the microchip. To facilitate the microchip design, electric fields generated from the microchip were first simulated using software, and experiments were conducted to validate the performance of the microchip. Yeast cells suspending in the 6-aminohexanoic acid (AHA) solution were used in this study, and the effects of the cell medium, the voltage input and the voltage frequency were analyzed. The results confirm that cell patterns are successfully created with the microchip and this microchip offers an easy method to fabricate cell patterns on a substrate for characterization.**

I. Introduction

Biological cells are the most fundamental unit of living organisms [1]. It is well known that culturing cells is challenging as they are very sensitive to different chemicals and the surrounding environment. In order to better understand their behaviors, laboratory technicians are required to carry out a large number of tests to study the cell behaviors and the testing process often involves lying cells uniformly on a plane substrate for easier assay and characterization. With advances in technology, robotics and automation can bring convenience to the tedious process.

To date, a number of techniques have been proposed for arranging and organizing cells on a plane substrate [2-5]. In general, these techniques can be cataloged into the contact micromanipulation and the non-contact micromanipulation [6]. For the contact manipulation system, a physical force would be generated only if the system reaches the object. For instance, Nagai et al. [7] proposed a traditional pick-and-place mechanism to manipulate cells with a robotic system. The micro-pipette was attached to an electrode to measure the electrical current in real time to avoid applying excessive suction pressure during cell handling. For those non-contact micromanipulation techniques, a field is always produced to remotely drive the particle. Hu et al. [8] employed a robotic optical tweezers system to arrange floating cells into a defined pattern. The optical beam was split into multiple beams to manipulate cells simultaneously. Okochi et al. [9] employed magnetic field for cell patterning. A pin holder consisting of multiple pillars were placed underneath of a plate to attract magnetically labeled cells. Collins et al. [10] employed acoustic wave to guide cell patterning in a microfluidic chip. Surface acoustic waves were applied at different frequencies to facilitate cell positioning on a piezoelectric substrate. Dura et al. [11] developed a microfluidic chip device to trap cells with respect to the fluid flow direction. Cell containing fluid can be injected at two sides of the traps to enable cell pairing for characterization. Although these techniques work well for their respective application, they also have several limitations, such as the limited throughput and the size of the cell pattern.

In recent years, dielectrophoresis has been studied extensively in various fields, including environmental research, chemistry, materials science, and biomedical research [12-15]. Dielectrophoresis is the use of non-uniform electric fields to induce motions on particles. Depending on the dielectric properties, particles are either attracted or repelled along the field gradients, and such phenomenon is also known as positive (p-DEP) or negative (n-DEP) dielectrophoresis. Since this technique does not require direct contact with the particles and the required hardware is relatively simple, its applications have been used for filtering, sorting and separation, characterization and diagnosis. For cell patterning, Hsiung et al. [16] employed electrode pairs for a uniform pattern of cells on an Indium Tin Oxide (ITO) coated glass slide. Albrecht et al. [17, 18] encapsulated cells patterned on the electrode via dielectrophoresis in a photosensitive material. Tsutsui et al. [19] and Lin et al. [20] employed the photosensitive material to define the mold for dielectrophoretic cell patterning. Among all these researches, p-DEP is widely employed because a higher DEP force could be generated for patterning. Nevertheless, cells are required to group and pattern onto the surface of the electrodes which have high electric field strengths, posing potential threats to the cell viability. Hence, there is a growing interest in cell patterning via n-DEP [14, 15], but many challenges exist to the development and characterization of an easy-to-fabricate device for cell patterning.

In this study, a microchip device employing the principle of negative dielectrophoresis is designed and fabricated. One key advantage of this microchip is that it can separate the cell pattern and the substrate on two different planes, offering higher flexibility in the patterning process. In order to generate sufficient DEP force for patterning, electric fields generated from the microchip were simulated and experiments were conducted to validate the performance of the microchip. A

The work was supported in part by the Research Grant Council of the Hong Kong Special Administrative Region, China, under Grant 25204016.

K. Huang, H. K. Chu*, B. Lu and L. Cheng are with the department of Mechanical Engineering, The Hong Kong Polytechnic University, Hong Kong. (*Corresponding Author, email: henry.chu@ polyu.edu.hk)

series of tests were conducted to examine the effects of different experimental parameters on the patterning efficiency.

This paper is outlined as follows: the design and the working principle of the microchip are given in Section II; the experimental setup is described in Section III; the results and discussions are provided in Section IV; and Section V summarizes the findings in this paper.

II. Design of the Microchip

A. Working Principle

The microchip employs negative dielectrophoresis to create a cell pattern on a substrate. The working principle is to utilize an electrode pair to generate non-uniform electric fields in the microenvironment between the microchip and the substrate. As described in Pohl [21], dielectric particles exposing in an alternating electric field are polarized. As the induced charge is not uniformly distributed over the particle surface, a macroscopic dipole is thus created. If the fields are not uniform, a net DEP force, F_{DEP} , acting on two sides of the particles, can be evaluated as:

$$F_{DEP}=2\pi r^3 \varepsilon_m \mathrm{Re}[K(\omega)]\nabla E^2 \quad (1)$$

where r is the particle radius, ε_m is the permittivity of the suspending medium, ∇ is the Del vector operator, E is the root mean square of electric field and Re[$K(\omega)$] is the real part of the Clausius-Mossotti (CM) factor. For viable cells, the particle can be modeled as a single-shell. By neglecting the conductance of the membrane, the CM factor is derived as [22]:

$$K(\omega)=\frac{\omega^2(\tau_m\tau_c^*-\tau_c\tau_m^*)-1+j\omega(\tau_m^*-\tau_m-\tau_c^*)}{2-\omega^2(2\tau_m\tau_c^*+\tau_c\tau_m^*)+j\omega(\tau_m^*+2\tau_m+\tau_c^*)} \quad (2)$$

where $\tau_c^*=\frac{C_m r}{\sigma_c}$, $\tau_c=\frac{\varepsilon_c}{\sigma_c}$, $\tau_m^*=\frac{C_m r}{\sigma_m}$, $\tau_m=\frac{\varepsilon_m}{\sigma_m}$, are time constants, C_m is the specific cell membrane capacitance, σ is the conductivity, and ε is the permittivity. The subscripts c and m stand for the cell and the medium. The sign of the CM factor is controlled by the dielectric properties of the cell and the medium, which are dependent on the frequency of the applied voltage, ω. A positive real part of the CM factor indicates the phenomenon of p-DEP while a negative real part indicates the phenomenon of n-DEP. In this work, experimental parameters were chosen to keep the real part in a negative value so that cells can be patterned onto the substrate.

B. Design and Fabrication of the Microchip

Within the microchip, an electrode pair is utilized to generate electric fields for cell patterning. In general, two electrode configurations are commonly employed in the field and they are the top-and-bottom [17-20], and the side-by-side fashion [13, 15, 23]. In this work, the microchip adopts the side-by-side electrode configuration, leaving the opposite side of the microchannel for substrate placement. When the electrode pair is connected to an AC voltage, circular electric field lines are formed, as shown in Fig 1. During the experiments, cells are injected from one side of the microchannel sandwiched between the microchip and the substrate. Due to the gravitational force (F_g), cells will gradually sink to the bottom of the substrate. Meanwhile, the energized electrode pair induce n-DEP force to drive the cells towards the center and underneath of the electrode, which has the lowest electric field.

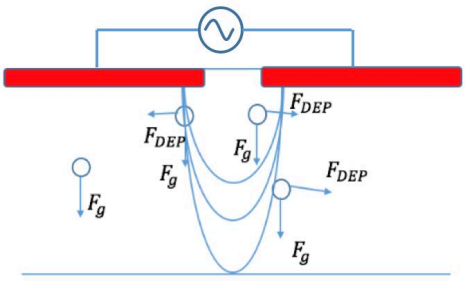

Fig. 1. Schematic Diagram showing the electric fields generated from a planar electrode

In order to create a uniform cell dot pattern, multiple electrode pairs, consisting of a circle electrode and a surrounding electrode, are incorporated in the microchip design. In order to minimize the design space and the connection, the surrounding electrodes are grouped into a common electrode. Based on the microchip layout, a 4-by-4 electrode array is proposed. In order to establish non-uniform electric fields in the microchannel, Multiphysics software, COMSOL, was used to simulate the results for analysis. In the simulation model, the circle electrodes were modeled as a circular disk while the surrounding electrode was modeled as a rectangular plane. The microchannel was set with a height of 100 μm that was filled with the medium. Figure 2 shows the simulation of the electric field formed by the microchip when a voltage was applied to the electrodes. The high electric field is represented by the regions in red, which is located at the gaps between the opposite electrodes. In contrast, the low electric field is represented by the regions in blue, which is located at the center of the circle electrode. The figures show that the non-uniform electric field is successfully established through the proposed electrode layout design. To explore the effect of the electrode size, a simulation was performed with larger and smaller circle electrodes. Comparing the results, the field strength generated from smaller electrodes is weaker. Also, the field distribution near the surrounding electrode is relatively uniform, and cells may not experience the DEP effect. Hence, reducing the electrode size will reduce the regions for cell manipulation.

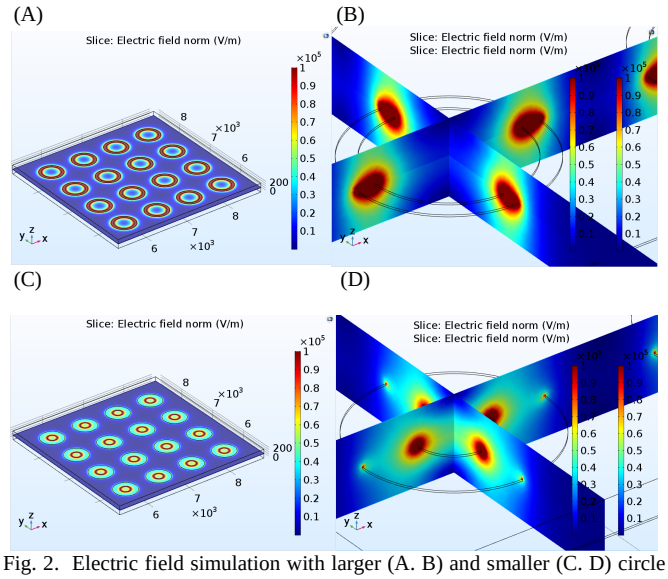

Fig. 2. Electric field simulation with larger (A. B) and smaller (C. D) circle electrodes. (A, C) Horizontal sectional view of the electric field simulation. (B, D) Two vertical cross-sectional plot of electric field simulation.

Based on the proposed electrode layout, a number of microfabrication technologies can be used for the fabrication, and standard Printed Circuit Board (PCB) fabrication is selected. Considering the manufacturing limitation, the center electrode is designed as a circle with a 200 μm in radius. The surrounding electrode is designed to have 16 holes, with a diameter of 700 μm on a 3.5 mm * 3.5 mm rectangular plane. To prevent the interaction effect between electrodes, the holes in the surrounding electrode are limited with a 100 μm distance. The PCB design illustration is shown in Fig. 3 using Altium Designer. To maintain the integrity of the microchip, a double-layer PCB was selected to provide higher design flexibility by utilizing both sides of the PCB board for electrode routing and layout (Shenzhen BitLand Information Technology Co., Ltd), and all electrodes can fit in one board without any overlapping issues.

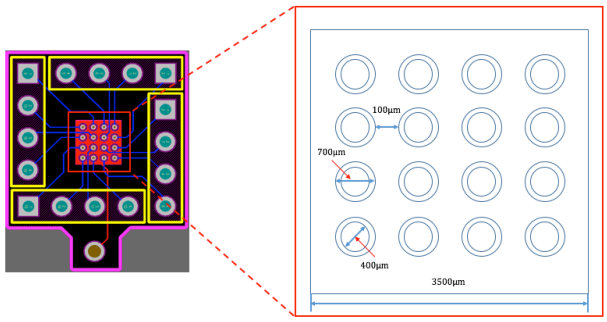

Fig. 3. Microchip schematic by Altium Designer.

III. Materials and Methods

A. Cell Medium Preparation

In this study, yeast cell was selected to examine the DEP phenomenon and the patterning efficiency. Actively dried yeasts, Saccharomyces cerevisiae, were re-activated in sugar solution with a concentration of 27 g/L and heated for 1 hour at a temperature of 35°C. To test the pattern effect of both live yeast cell and dead yeast cell, the solution containing the yeast cells were divided into two parts. Half of them was heated at a temperature of 90°C to prepare the dead yeast cells. Dead yeast cells were stained by Janus green B (Shanghai MAIKUN Chemical Co., Ltd) to get a better image contrast for view under the microscope. The cells were re-suspended in DI water and 1M AHA solution (Ruibio) for the experiments.

B. Experiment Setup

The system consists of five main components: a Leica inverted microscope, a dual syringe pump, a function generator, a microchip, and a slice of the glass substrate, as shown in Fig.4. Two 100 μm spacers were sandwiched between the microchip and the glass substrate to create a microchannel for the cell solution to flow through. The syringe pump was used to inject the cell containing medium, and the function generator was used to provide the voltage for electric field generation. The formation of the cell pattern was observed through the Leica inverted microscope.

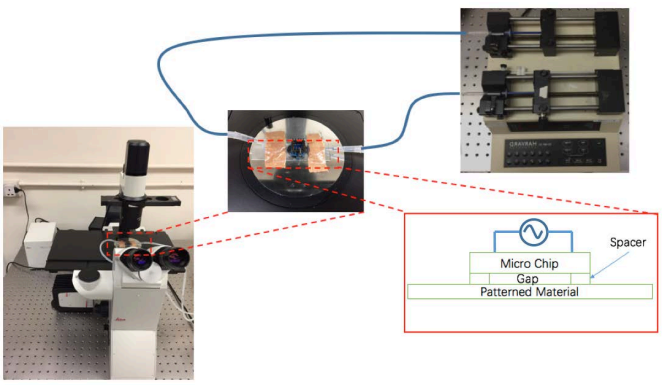

Fig. 4. Experimental Setup

IV. Results and Discussion

The microchip was used to create different cell patterns, and a series of experiments were conducted to evaluate the performance and efficiency of the microchip with different experimental parameters. First, the effects of the medium used for the experiments were examined. Then, different signal voltages were applied to create the cell patterns and the results were compared to the simulation findings. Finally, different voltage frequencies were applied to evaluate the crossover frequency, which the phenomenon is changed from p-DEP to n-DEP, and the frequency range suitable for the experiments.

A. Medium

As discussed, the properties of the suspension medium have a direct impact on successful cell patterning via the microchip. The relative dielectric properties between the cells and the medium determine the sign of the DEP force. Also, the motions of the cells are also linked to the medium. To test the effect, dead yeast cells were suspended in DI water and 1M AHA solution, respectively. The cell solutions were first pumped to completely fill the channel, and the voltage was applied to the electrodes. After 3 minutes of operation, the cell pattern was observed through the microscope.

The results in Fig. 5 show that in AHA solution, cells floating in the medium were chained together and manipulated towards the center of the circle electrode. In contrast, in DI water, the DEP effect was not obvious, and cells remained floating in the microchannel. According to Eq(1), the DEP

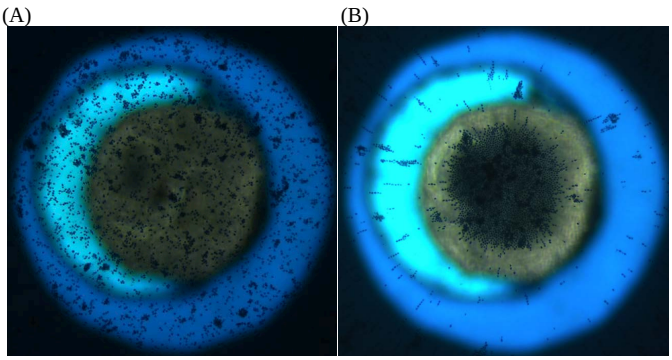

Fig. 5. Phenomenon of DEP Effect for dead yeast cells suspended in different medium (A) DI water. (B) 1M AHA solution

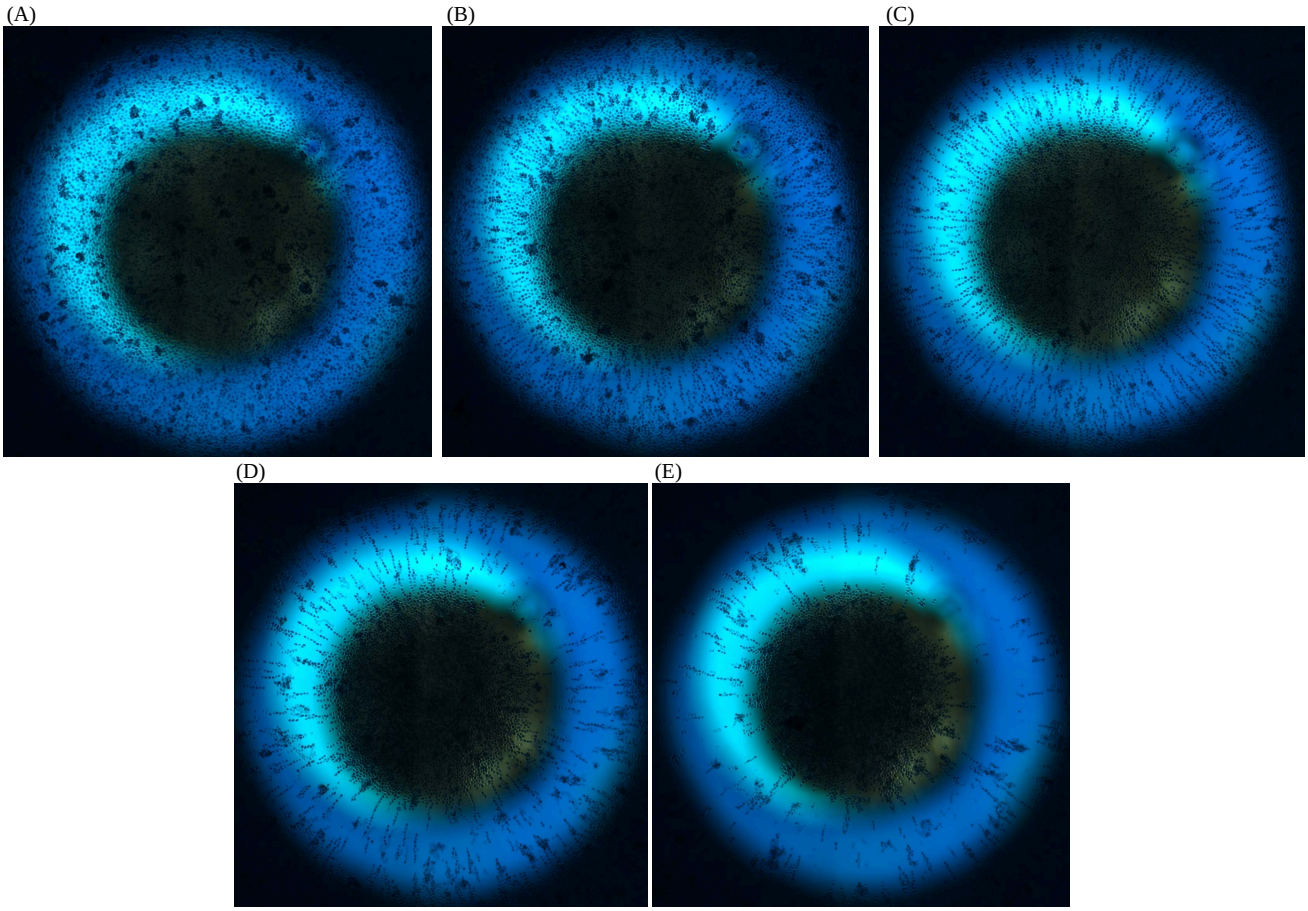

Fig. 6. Phenomenon of DEP Effect for yeast cells with different signal voltage. (A) 2V. (B) 4V. (C) 6V. (D) 8V. (E) 10V.

force is dependent on the relative permittivity of the medium. Although AHA solution has a higher ε_m value (160) then DI water (78), the induced forces were not sufficient to manipulate the cells. One observation from the experiments was that in DI water, the majority of the cells quickly sunk into the bottom (substrate). As cells were settled on the substrate surface, the adhesion force between the cell and the substrate dominates over the DEP force and cells were unable to form any cell pattern.

B. Voltage Input

The size of the cell dot that the microchip can be created is important to evaluate the performance of the chip. Given that the number of cells in the medium is fixed, a larger cell dot indicates that the microchip is more effective to utilize the surrounding cells to form the pattern at the center of the electrode. According to Eq (1), the strength of the force is proportional to the gradient of the square of the electric field. To explicitly examine the effect of this parameter, voltage

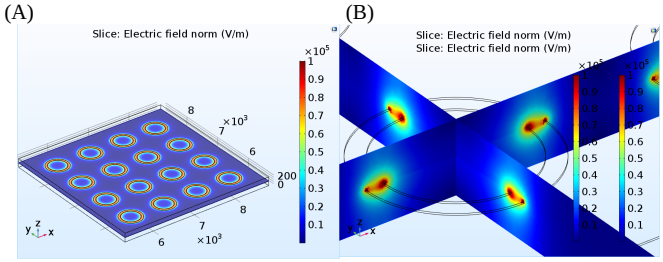

Fig. 7. (A) Horizontal sectional view of the electric field simulation. (B) Two vertical cross-sectional plot of electric field simulation.

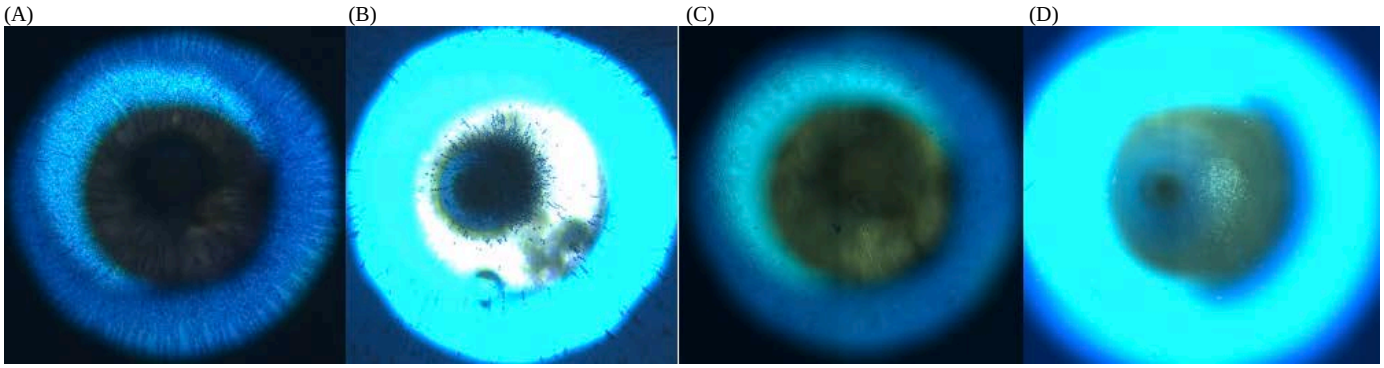

Fig. 8. Phenomenon of DEP Effect for yeast cells in AHA solution (A) dead yeast cell with p-DEP effect. (B) dead yeast cell with n-DEP effect. (C) live yeast cell with p-DEP effect. (D) live yeast cell with n-DEP effect.

inputs of 2V, 4V, 6V, 8V, and 10V were applied to the microchip. The signal frequency was set at 6MHz and the effects on dead yeast cells in 1M AHA solution were shown in Fig. 6. As expected, when the voltage input is low, cells that are far away from electric fields cannot be manipulated due to the generation of a weaker DEP force. As the voltage continues to increase, cell chains are formed along the radial direction and the size of the cell dot is growing, as shown in the figure. At a higher voltage, cells clustering at the center of the electrode become more obvious. It can be noticed that most of the cells suspending at the gap between the circle electrode and the surrounding electrode are manipulated to form the cell pattern, leaving a clear (cell-free) medium at the gap.

The effect of the voltage input was also simulated using the software. Comparing Fig. 3 and Fig. 7, using a low voltage input will lead to a more uniform electric field distribution, especially near the center of the electrode. Hence, it supports the result that the dot size is dependent on the voltage input.

C. Voltage Frequency

According to Eq (2), the frequency is the most important parameter determining the polarity (positive or negative) of the DEP force. This equation Using Eq (2) and substituting the parameters with values listed in Table I [15], the CM factor for live and dead yeast cells in 1.0 M AHA solution was simulated using MatLAB. The frequency range was set from 20 Hz to 300 MHz and the simulation results were summarized in Table II.

Fig. 8 illustrates the DEP effects of the dead yeast cells (blue) and the live yeast cells (transparent) under a single dot electrode at various frequencies. When signals of 5MHz and 30MHz were supplied to dead and live yeast cells, respectively, cells were gathered together to form cell chains and migrated towards the center of the dot electrode, which can be explained as the n-DEP phenomenon (Figs. 8(B and D)). If a 1MHz signal was applied to the electrodes, both live and dead yeast cells were concentrated in the gap between the electrodes, indicating the p-DEP effect (Figs. 8(A and C)). By changing the voltage frequency through the function generator, the crossover frequencies of dead and live yeast cells, which are the turning points from negative to positive CM factor, are found to be 3.5 MHz and 16 MHz, respectively. Comparing the results, there are discrepancies between the experiments and the simulations on the crossover frequency. For both live and dead yeast cells, the simulation results show that the crossover frequencies are in the region of 100MHz, higher by an order of magnitude. The simulation values are comparable to the one (10^8 Hz) reported in [24] and [25], suggesting the single-shell model may not be appropriate to describe yeast cells in AHA solution. Other cell models, such as two-shell [26] or multi-shell model [27], should also be considered to evaluate the optimal cell model to best describe yeast cells. Despite the discrepancy, the crossover frequency can be obtained through experiments and cell patterning via n-DEP can be performed with a usable frequency. It is known that the crossover frequency is unique to each cell type and the medium, but similar tests can be performed on different cell types to obtain the suitable frequency range for the experiments.

TABLE I: PROPERTIES OF YEAST CELL

Symbol	Quantity	Value
R	Cell radius	2.15 μm
ε_c	Internal relative permittivity	50.6 ε_0
σ_c	Internal conductivity	0.515 S/m
C_m	Membrane capacitance	7.03 F/cm^2

TABLE II: Simulation results of the CM factor (sign) for live and dead yeast cells in AHA solution at different frequencies

Frequency	20kHz	100kHz	1MHz
DEP Effect of Live Yeast Cell	-	+	+
DEP Effect of Dead Yeast Cell	+	+	+
Frequency	5MHz	30MHz	300MHz
DEP Effect of Live Yeast Cell	+	+	-
DEP Effect of Dead Yeast Cell	+	+	-

V. CONCLUSION

In this study, a microchip consisting of a 4-by-4 dot electrode array was designed and fabricated for cell patterning. This microchip employed n-DEP and cell patterns were created on a substrate lying on the microchip surface. The microchip was fabricated using the PCB technique, and its performance was examined through experiments using yeast cells. Results show that the AHA solution is effective to minimize the amount of cells sunk to the bottom. When a higher voltage is used, a larger cell dot can be created. Also, the usable frequency from a function generator can induce p-DEP and n-DEP force on live and dead yeast cells, and a suitable frequency for the experiments can be selected accordingly. This microchip provides an easy and simple method to create cell patterns on a substrate to facilitate cell assay and characterization.

REFERENCES

[1]. C. A. Vacanti, "History of tissue engineering and a glimpse into its future," *Tissue engineering,* vol. 12(5), pp. 1137-1142, 2006.
[2]. T. Yasukawa *et al.*, "Electrophoretic cell manipulation and electrochemical gene-function analysis based on a yeast two-hybrid system in a microfluidic device," *Analytical chemistry,* vol. 80(10), pp. 3722-3727, 2008.
[3]. K. Ino, A. Ito, and H. Honda, "Cell patterning using magnetite nanoparticles and magnetic force," *Biotechnology and Bioengineering,* vol. 97(5), pp. 1309-1317, 2007.
[4]. J. El-Ali, P. K. Sorger, and K. F. Jensen, "Cells on chips," (in eng), *Nature,* vol. 442(7101), pp. 403-11, Jul 27 2006.
[5]. H. Chu, Z. Huan, J. Mills, J. Yang, and D. Sun, "Three-dimensional cell manipulation and patterning using dielectrophoresis via a multi-layer scaffold structure," *Lab on a Chip,* vol. 15(3), pp. 920-930, 2015.
[6]. R. Amit, A. Abadi, and G. Kosa, "Characterization of steady streaming for a particle manipulation system," *Biomedical microdevices,* vol. 18(2), p. 39, 2016.
[7]. M. Nagai, K. Kato, K. Oohara, and T. Shibata, "Pick-and-Place Operation of Single Cell Using Optical and Electrical Measurements for Robust Manipulation," *Micromachines,* vol. 8(12), p. 350, 2017.
[8]. S. Hu and D. Sun, "Automatic transportation of biological cells with a robot-tweezer manipulation system," *The International Journal of Robotics Research,* vol. 30(14), pp. 1681-1694, 2011.
[9]. M. Okochi, S. Takano, Y. Isaji, T. Senga, M. Hamaguchi, and H. Honda, "Three-dimensional cell culture array using magnetic force-based cell patterning for analysis of invasive capacity of BALB/3T3/v-src," *Lab on a chip,* vol. 9(23), pp. 3378-3384, 2009.
[10]. D. J. Collins, B. Morahan, J. Garcia-Bustos, C. Doerig, M. Plebanski, and A. Neild, "Two-dimensional single-cell patterning with one cell per well driven by surface acoustic waves," *Nature communications,* vol. 6, p. 8686, 2015.

[11]. B. Dura *et al.*, "Profiling lymphocyte interactions at the single-cell level by microfluidic cell pairing," *Nature communications*, vol. 6, p. 5940, 2015.
[12]. Z. R. Gagnon, "Cellular dielectrophoresis: applications to the characterization, manipulation, separation and patterning of cells," *Electrophoresis*, vol. 32(18), pp. 2466-2487, 2011.
[13]. B. Yafouz, N. A. Kadri, and F. Ibrahim, "The design and simulation of a planar microarray dot electrode for a dielectrophoretic lab-on-chip device," *International Journal of Electrochemical Science*, vol. 7(12), pp. 12054-12063, 2012.
[14]. M. Suzuki, T. Yasukawa, H. Shiku, and T. Matsue, "Negative dielectrophoretic patterning with colloidal particles and encapsulation into a hydrogel," *Langmuir*, vol. 23(7), pp. 4088-4094, 2007.
[15]. K. Ino, H. Shiku, F. Ozawa, T. Yasukawa, and T. Matsue, "Manipulation of microparticles for construction of array patterns by negative dielectrophoresis using multilayered array and grid electrodes," *Biotechnology and bioengineering*, vol. 104(4), pp. 709-718, 2009.
[16]. L.-C. Hsiung *et al.*, "A planar interdigitated ring electrode array via dielectrophoresis for uniform patterning of cells," *Biosensors and Bioelectronics*, vol. 24(4), pp. 869-875, 2008.
[17]. D. R. Albrecht, R. L. Sah, and S. N. Bhatia, "Geometric and material determinants of patterning efficiency by dielectrophoresis," *Biophysical Journal*, vol. 87(4), pp. 2131-2147, 2004.
[18]. D. R. Albrecht, V. L. Tsang, R. L. Sah, and S. N. Bhatia, "Photo-and electropatterning of hydrogel-encapsulated living cell arrays," *Lab on a Chip*, vol. 5(1), pp. 111-118, 2005.
[19]. H. Tsutsui *et al.*, "Efficient dielectrophoretic patterning of embryonic stem cells in energy landscapes defined by hydrogel geometries," *Annals of biomedical engineering*, vol. 38(12), pp. 3777-3788, 2010.
[20]. R. Z. Lin, C. T. Ho, C. H. Liu, and H. Y. Chang, "Dielectrophoresis based ‐ cell patterning for tissue engineering," *Biotechnology Journal: Healthcare Nutrition Technology*, vol. 1(9), pp. 949-957, 2006.
[21]. H. A. Pohl, "Dielectrophoresis," *The behavior of neutral matter in nonuniform electric fields*, 1978.
[22]. T. Jones, "Electromechanics of ParticlesCambridge Univ," *Press, Cambridge*, 1995.
[23]. B. Yafouz, N. A. Kadri, and F. Ibrahim, "Dielectrophoretic manipulation and separation of microparticles using microarray dot electrodes," *Sensors*, vol. 14(4), pp. 6356-6369, 2014.
[24]. G. Mernier, N. Piacentini, R. Tornay, N. Buffi, and P. Renaud, "Cell viability assessment by flow cytometry using yeast as cell model," *Sensors and Actuators B: Chemical*, vol. 154(2), pp. 160-163, 2011.
[25]. S.-Y. Tang, W. Zhang, S. Baratchi, M. Nasabi, K. Kalantar-zadeh, and K. Khoshmanesh, "Modifying dielectrophoretic response of nonviable yeast cells by ionic surfactant treatment," *Analytical chemistry*, vol. 85(13), pp. 6364-6371, 2013.
[26]. Z. Gagnon, J. Mazur, and H.-C. Chang, "Integrated AC electrokinetic cell separation in a closed-loop device," *Lab on a Chip*, vol. 10(6), pp. 718-726, 2010.
[27]. S. Gupta, R. G. Alargova, P. K. Kilpatrick, and O. D. Velev, "On-chip electric field driven assembly of biocomposites from live cells and functionalized particles," *Soft Matter*, vol. 4(4), pp. 726-730, 2008.